



HAL
open science

Integrated process for production of surfactin Part 1: Adsorption rate of pure surfactin onto activated carbon

Tao Liu, Ludovic Montastruc, Frédérique Gancel, Ling Zhao, Iordan Nikov

► **To cite this version:**

Tao Liu, Ludovic Montastruc, Frédérique Gancel, Ling Zhao, Iordan Nikov. Integrated process for production of surfactin Part 1: Adsorption rate of pure surfactin onto activated carbon. *Biochemical Engineering Journal*, 2007, 3 (3), pp.333-340. 10.1016/j.bej.2007.01.025 . hal-03594255

HAL Id: hal-03594255

<https://hal.science/hal-03594255>

Submitted on 2 Mar 2022

HAL is a multi-disciplinary open access archive for the deposit and dissemination of scientific research documents, whether they are published or not. The documents may come from teaching and research institutions in France or abroad, or from public or private research centers.

L'archive ouverte pluridisciplinaire **HAL**, est destinée au dépôt et à la diffusion de documents scientifiques de niveau recherche, publiés ou non, émanant des établissements d'enseignement et de recherche français ou étrangers, des laboratoires publics ou privés.

Integrated process for production of surfactin

Part 1: Adsorption rate of pure surfactin onto activated carbon

Tao Liu^a, Ludovic Montastruc^b, Frédérique Gancel^b, Ling Zhao^a, Jordan Nikov^{b,*}

^a State Key Laboratory of Chemical Engineering, East China University of Science and Technology, Shanghai, PR China

^b Laboratoire ProBioGEM EA 1026, Polytech'Lille, USTL, Lille, France

Abstract

The work reported in this paper is aimed at studying the adsorption of surfactin from aqueous solution onto activated carbon. Among the factors, agitation rate, activated carbon particle-size, pH, temperature, initial adsorbate concentration, adsorbent amount and ionic strength of the solution were studied. Both adsorption equilibrium and kinetics showed that activated carbon acted as a suitable adsorbent for surfactin recovery. Two mechanisms represented by different kinetic models were examined, namely, the intraparticle diffusion one and the one involving chemisorption accompanied by surface coverage (conforming to the Elovich concept).

Keywords: Surfactin; Integrated processing; Adsorption; Modelling; Kinetic parameters

1. Introduction

Surfactin, a bacterial lipopeptide produced biologically by *Bacillus subtilis* [1], is one of the most widely studied biosurfactants and reduces the surface tension of water from 72 to ~30 mN/m at concentrations of ~10 mg/L [2–4]. Surfactin commonly has the advantages of biodegradability, low toxicity and biocompatibility over chemically synthesized surfactants [4–6]. As a result, it has been found an attractive alternative or supplement to chemically synthesized surfactants that have a detrimental effect on the environment and successful application in areas such as bioremediation [4,7] and oil recovery [5,8,9].

However, biosurfactants are not widely available because of their high production cost, which results primarily from low strain productivities and high recovery expenses. Many efforts have been made to improve the productivities [10–12]. The most widely used approaches for recovery and purification of biosurfactants involve precipitation at extreme pH and extraction with organic solvents [13]. However, this process usually leads to release of hazardous wastes and high cost as well. Several other new methods such as application of foaming [14] and ultrafiltration [15,16] were applied for surfactin recovery. However, the

“foaming technique” is not applicable in continuous processing, since at gas supply, the presence of surfactin generates extensive foaming that imposes difficulties on the bioreactor performance. Foaming evolution causes liquid outflow and changes substrate and cells concentration. In particular, the valid reactor volume decreases and the process become hard to control [14]. In order to avoid these drawbacks, while using an integrated approach, the product may be removed from the reactor during its formation by the procedure known as in situ product removal (ISPR). For example, several integrated bioprocesses have been proposed to optimise productivity and cost-effectiveness of low and high molecular weight molecules [17]. Thus, in view of continuous surfactin production, we propose a new fermentation process comprising a bioreactor, a microfilter and an adsorption column, as shown in Fig. 1.

The microfilter is added for cell recovery before the adsorption column. The permeate flow containing no cells enters the adsorption column whereas the retentate flow containing cells flows back into the fermentation reactor. The adsorption column is designed as a fixed bed of activated carbon. This one represents a new application for surfactin recovery of and foam elimination. Among the advantages of such integrated process is the direct surfactin removal from the crude fermentation medium by the adsorption/desorption technique that is most promising from industrial point of view. Using concepts of adsorption theory [18–20] it is well known that, to interpret the applicability of

* Corresponding author. Tel.: +33 3 28 76 74 10; fax: +33 3 28 76 74 01.
E-mail address: Jordan.Nikov@polytech-lille.fr (I. Nikov).

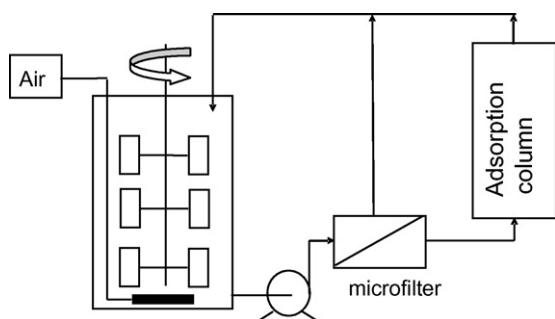


Fig. 1. The integrated fermentation process including the adsorption unit.

this technique properly one has to determine the individual steps of the adsorption process governing the overall removal rate in the system. The rate-limiting step is important from the point of view of column design. On the other hand, the adsorption kinetics should be studied at low surfactin concentration, corresponding to its removal during its formation. According to the literature, film or pore diffusion are the major rates controlling steps of sorption from the solution to the porous sorbents. Since they act in series [20], the slower of the two steps would be the rate limiting one of the adsorption processes [21].

The kinetic study presented in this work has been considered as part of a larger investigation of separation efficiency of commercial activated carbon particles towards surfactin separation from real fermentation media. The effects of various variables, such as agitation rate, activated carbon particle-size, pH and temperature of the solution, initial adsorbate concentration, adsorbent amount and the solution ionic strength on the adsorption rate and equilibrium were examined. In a further development, both the intraparticle diffusion model and the Elovich model were applied for mechanistic analysis of the adsorption rates.

2. Experiments

2.1. Materials (bacterial strain and culture medium, adsorbent and aqueous solution)

The surfactin was produced by *B. subtilis* ATCC 21332. The bioconversion based on *B. subtilis* ATCC 21332 reached 0.8 g surfactin/L culture at the end of the fermentation [22,23]. Cultures from the late exponential growth phase were harvested and used as inoculums in the surfactin fermentation experiments. The culture optical density was determined at 600 nm. The culture was washed and concentrated 10 times by centrifugation. The seed cultures were inoculated into 1000 mL flasks containing 200 mL of Landy medium [23] in order to obtain initial optical density 0.5. The batch cultures were incubated at 37 °C and pH at ~7 at an agitation rate of 200 rpm. The cell growth and surfactin concentration were monitored.

Merck activated carbon (Ref. 1.02514.1000) with an approximately spherical geometry was used as adsorbent. The activated carbon particles used were sieved to obtain fractions of average size 1.40, 0.90, 0.72, 0.56 and 0.45 mm. The specific surface of the activated carbon was determined to be 960 m²/g.

A buffer solution composed of potassium hydrogen phosphate (0.2 mol/L of K₂HPO₄) and potassium di-hydrogen phosphate (0.2 mol/L of KH₂PO₄) were used as to control pH in between 6.0 and 8.5, as tested by InoLab pH/ION Level 2 P (WTW GmbH & Co. KG, Germany).

2.2. Experimental procedures for adsorption

In each adsorption experiment, an amount of activated carbon (0.025–0.1 g) and buffer solution of 20 mL were placed in a 200 mL flask, into which the amount of surfactin solution was added. Then, the flask was laid in a controlled environment incubator shaker (New Brunswick Scientific Co., USA). Following the adsorption, the aqueous samples taken out at selected intervals were applied to an Alltech C₁₈ cartridge (Ref. 1205250, 500 mg/4 mL), that had been rinsed in advance with 20 mL HPLC grade methanol and 8 mL ultra pure water. Further, the surfactin retaining cartridge was rinsed successively by using 8 mL ultra pure water. Finally, the surfactin was eluted off the cartridge with 6 mL HPLC grade methanol. Fifty percent aqueous methanol was not applied to rinse the cartridge according to reference [24] because the HPLC results showed that it also eluted the surfactin in the cartridge. The eluate was evaporated by using a vacuum centrifuge, while the residue was dissolved in 0.2 mL of HPLC grade methanol for subsequent HPLC. Table 1 gives the range of operating conditions used in the kinetic study.

2.3. Quantitative analysis of surfactin

The surfactin concentration in the methanol solution was determined by reverse phase C₁₈ HPLC (600 s, Waters, USA) equipped with a Merck C₁₈ column (5 μm, Merck, Germany). The standard of surfactin was purchased from Sigma (USA). The product was synthesized by *B. subtilis* and is 98% pure. The solution concentration was adjusted to obtain 500 mg/L in 20 μL in each injection sample. The surfactin was eluted during 20 min under ACN/H₂O/TFA (80% of acetonitrile, 20% of water, 0.1% of trifluoroacetic acid, v/v/v) at 1 mL/min. The spectrum was analysed using values of second derivative. As shown in Fig. 2a, seven major peaks appeared in the standard HPLC UV-spectrum of surfactin. They were selected through calibration. Surfactin substance gives its major peak at 212–213 nm associated with a minor peak shown in the same figure.

The quantification of surfactin from real medium is somewhat complex since surfactin has a number of isomers [25]. *B. subtilis* synthesized heptapeptides interlinked with a β hydroxyacid containing 13–15 C in the *n*, *iso* or *anteiso* configuration. Several peptides' variants usually coexist in the same extract [6]. The peaks used in surfactin calculation are illustrated in Fig. 2b.

The amount of adsorption at equilibrium, q_e (mg/g), was calculated by

$$q_e = \frac{C_0 - C_e}{m} \quad (1)$$

Table 1
Experiments conditions

Agitation rate (rpm)	Initial concentration (mg/L)	Adsorption time	Temperature (°C)	pH	Adsorbent amount (g/L)	Adsorbent diameter (mm)	Comments
80, 130, 180	19.0	2, 4 h	30	6.5	2.5	1.40	Agitation effect
130	19.0	0–3 h 0–4 h 0–4 h 0–4 h 0–14 h	30	6.5	5	0.45 0.56 0.72 0.90 1.40	Adsorbent diameter
130	19.0	0–20 h	30	6, 8.5	5	1.40	pH
130	19.0	7 days 4 days 3 days	20 30 40	6.5	5	1.40	Temperature on adsorption capacity
130	19.0	0–14 h 0–14 h 0–8 h 0–6 h	20 30 40 50	6.5	5	1.40	Temperature on adsorption rate
130	38, 19, 8.5	0–32 h	30	6.5	5, 2.5, 1.25	1.40	Adsorbent amount effect
130	19 7.5	0–14 h 0–8 h	30	6.5	5	1.40	Initial concentration effect

where C_0 and C_e are the initial and equilibrium liquid-phase surfactin concentrations, respectively (mg/L) and m is the amount of activated carbon used (g/L).

In the kinetic studies, the amount of adsorption at time t , q_t (mg/g), was calculated similarly by

$$q_t = \frac{C_0 - C_t}{m} \quad (2)$$

where C_t (mg/L) is the liquid-phase surfactin concentration at time t .

Some preliminary experiments to determine the reproducibility of our results have been realized. Because of the long time of the experiments (e.g. about 30 h per single point of a curve), Fisher's test was not applied. The preliminary results were completely satisfactory. For example, at the experimental conditions of Fig. 6, following four parallel experiments for each point, the mean deviation was lower than 7%. It is noteworthy that in the HPLC analyses at each point, subject to analysis has been all the amount of the fermentation liquid; thus, no liquid sampling has been practiced.

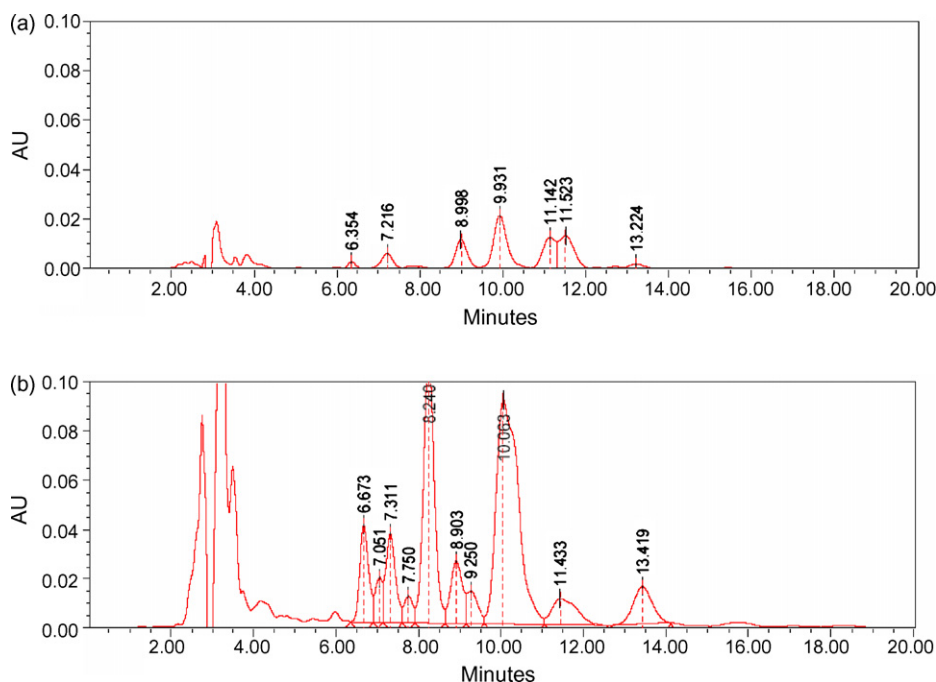


Fig. 2. HPLC spectrograms of standard surfactin (a) and surfactin obtained in this work (b). Seven peaks were used to calculate the amount of surfactin.

3. Results and discussion

3.1. Effect of agitation rate on adsorption

In order to verify that the external transport is rate-limiting step, surfactin adsorption runs have been carried out for 2 and 4 h at agitation rates of 80, 130 and 180 rpm. The agitation rate refers to a shaker and not to a stirrer. The initial concentration of surfactin was 19.0 mg/L. The temperature was 30 °C, pH of the aqueous solution was 6.5 and the amount of activated carbon was 2.5 g/L. In the case of 2 h adsorption at agitation rates of 80, 130 and 180 rpm, the residual surfactin was 12.0, 12.2 and 12.1 mg/L, respectively. While, in case of 4 h adsorption the three agitation rates the residual surfactin was 10.7, 10.8 and 10.7 mg/L. Referring to the range of agitation rates between 80 and 180 rpm, the results indicate that the external transport of surfactin from the aqueous solution to the adsorbent surface is too fast to represent the rate-limiting step of the overall adsorption. Therefore, we used 130 rpm as the agitation rate for surfactin adsorption in the further experiments.

3.2. Effect of activated carbon particle-size on the adsorption rates

In order to verify if the internal transport represented the rate-limiting step, surfactin adsorption on activated carbon was tested also by using carbon of different particle-size, between 0.45 and 1.40 mm, as shown in Fig. 3. The temperature was 30 °C and the amount of activated carbon was 5 g/L. As appears from Fig. 3, the smaller the activated carbon particles used, the faster the adsorption rate was. The initial adsorption rate corresponding to different particle-size of the activated carbon was calculated in parallel by using the initial surfactin concentration and the surfactin remaining following a 0.5 h adsorption. Fig. 4 depicts the dependence of initial adsorption rates on adsorbent particle-size. While decreasing the adsorbent particle-size, the initial adsorption rate would increase indicating that the intraparticle transport of surfactin controls the overall adsorption rate, provided that the

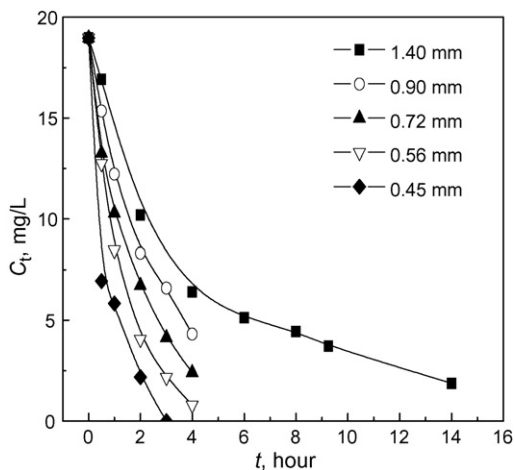


Fig. 3. Rates of surfactin adsorption onto activated carbons of different size ($T=30\text{ }^{\circ}\text{C}$, pH 6.5 and activated carbon 5 g/L).

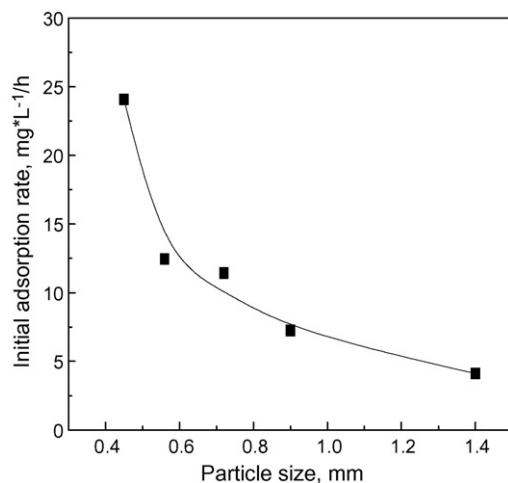


Fig. 4. Initial adsorption rates vs. activated carbon particle-size ($T=30\text{ }^{\circ}\text{C}$, pH 6.5 and amount of activated carbon 5 g/L).

effects of external transport have been eliminated. The smaller the activated carbon particles, the more difficult it is to collect them. In further studies, activated carbon with particle-size of 1.40 mm has been used.

3.3. Effect of pH on adsorption

Referring to surfactin fermentation, pH of the fermentation broth is generally maintained at 6–8.5. When pH of the broth is lower than 6, surfactin precipitates and production yield is lower. On the other limit, no fermentation takes place at pH higher than 8.5. A comparative experiment was carried out to test if surfactin adsorption rates would be affected by pH in the range pH 6–8.5. The amount of activated carbon used was 2.5 g/L. The adsorption rates of surfactin in the two buffer solutions with different pH agree with each other very well (the average deviation being lower than 0.15 mg/L), indicating that surfactin adsorption would not be affected by pH in the range 6.5–8.5 (data not shown). In further experiments, the buffer solution with pH 6.5 has been used. This result shows that the electrical properties, respectively, the zeta potential, of surfactin have any effect on the adsorption phenomena in the considered range in opposite to heavy metal removal process [4].

3.4. Effect of temperature on adsorption

Fig. 5 shows the isotherms of surfactin adsorption at 20, 30 and 40 °C, respectively. Preliminary experiments showed that adsorption was complete within 6 days at 20 °C, 3 days at 30 °C and 2 days at 40 °C. In order to obtain the equilibrium points, the experiments were performed in a shaker bath at 130 rpm for 7 days at 20 °C, 4 days at 30 °C and 3 days at 40 °C. The adsorption capacities of carbon for surfactin at 20, 30 and 40 °C were 39, 28 and 18 mg/g, respectively. Increasing the temperature, the adsorption capacity of surfactin would decrease. Fig. 6 shows the adsorption rates of surfactin at different temperatures, e.g. 20, 30, 40 and 50 °C, respectively. The concentration and the average particle-size of the activated carbon used were 5 g/L

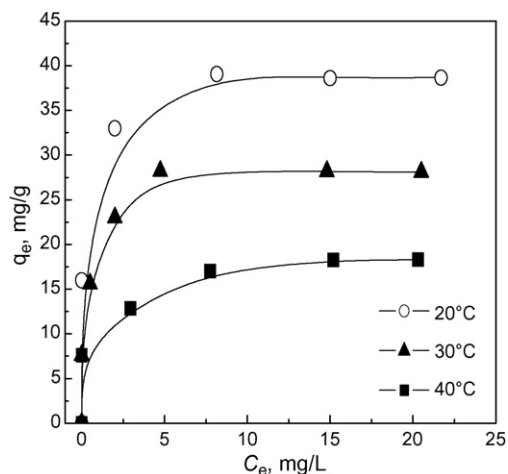


Fig. 5. Isotherms of surfactin adsorption onto activated carbon.

and 1.4 mm. It is seen that while increasing adsorption temperature the adsorption rate became faster. At 20 and 30 °C, the adsorption could not reach the equilibrium in 14 h. This result allows controlling the adsorption process using the temperature parameter.

3.5. Effect of surfactin initial concentration on adsorption

Fig. 7 shows the adsorption rates at different surfactin initial concentrations. The temperature was 30 °C and the average particle-size of the activated carbon used was 1.40 mm. Although surfactin concentrations were different, Fig. 7a shows that the ratio of the initial concentration to the amount of activated carbon remained nearly constant, i.e. about 7.5 mg (surfactin)/g (adsorbent) (this ratio is obtained by dividing the initial surfactin concentration by the adsorbent dose). During the initial adsorption period, the higher the surfactin concentration, the faster the adsorption rate was. While decreasing surfactin concentration in the liquid-phase, the adsorption rate of surfactin onto the activated carbon became increasingly slower. Referring to the adsorption process at different initial surfactin concentration maintaining similar ratio of the initial concentra-

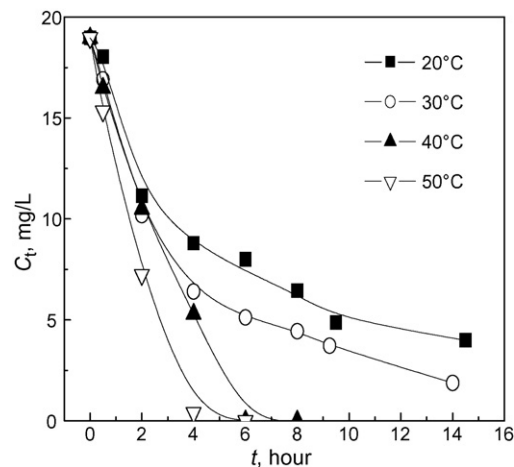


Fig. 6. Surfactin adsorption rates at different temperatures, pH 6.5, activated carbon concentration 5 g/L and carbon particle size = 1.40 mm.

tion to the amount of adsorbent, it seems that it takes the same time to reach final ‘equilibrium’. Fig. 7b illustrates the adsorption rates at different initial surfactin concentration compared to the critical micelle concentration (CMC). The amount of adsorbent is the same (5 g/L). In this figure, it is interesting to find that the adsorption rates at different initial surfactin concentrations, higher and lower than its critical micelle concentration (CMC) are identical. Using the relationship of surface tension and surfactin concentration The CMC value obtained at operating conditions of this study, namely 30 °C at pH 7, was ~5.23 g/L [26]. The result suggests the applicability of a nonlinear theoretical approach concerning the kinetics of adsorption on the porous surface of a micellar surfactant solution (e.g. see Danov et al. [27]). In the bulk, the micelles form a dynamic equilibrium with the monomers. In fact, it is proposed that, both monomers and micelles are involved in diffusion from the bulk to the solid surface accompanied by mass exchange between the two species. In the vicinity of an expanded adsorption subsurface layer (monolayer), the micelle releases monomers in order to restore the equilibrium surfactant concentration on the surface and in the bulk. Thus, only monomers are adsorbed.

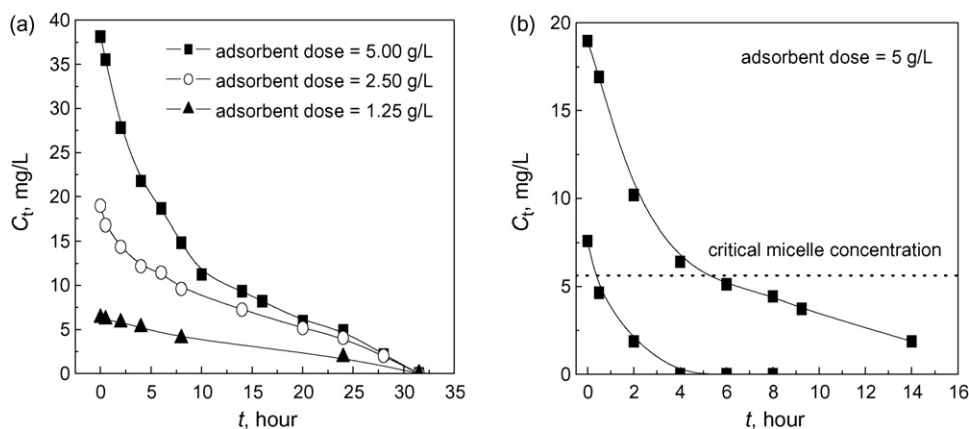


Fig. 7. Surfactin adsorption at different initial surfactin concentrations and amount adsorbent ($T=30\text{ }^{\circ}\text{C}$ and $\text{pH}6.5$).

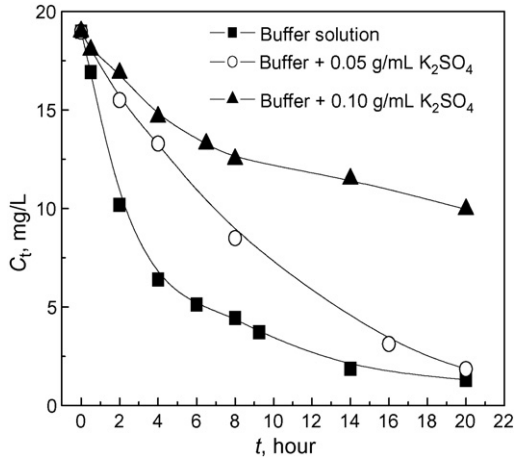


Fig. 8. Surfactin adsorption in three different solutions ($T=30^{\circ}\text{C}$, $\text{pH } 6.5$ and amount of activated carbon 5 g/L).

3.6. Effect of the ionic strength on the adsorption

Fig. 8 shows the adsorption rates of surfactin in the aqueous solutions of different ionic strength controlled by adding some K_2SO_4 . The temperature was 30°C and the concentration of the activated carbon was 5 g/L . The initial surfactin concentration was 19.0 mg/L . For the control solution and for the

buffer solution with $0.05\text{ g/mL K}_2\text{SO}_4$ it is shown that adsorption reaches similar equilibrium at similar process duration, though the adsorption rates are different. However, with regard to the buffer solution with added $0.1\text{ g/mL K}_2\text{SO}_4$, it appeared that the adsorption rate was slow and the carbon adsorption capacity of surfactin had decreased too.

3.7. Adsorption rate mechanistic analysis

The data obtained in this work indicates that the external transport is too fast to represent the rate-limiting step of the overall adsorption, but the effective diffusion may control the overall rate of the process. In order to identify adsorption mechanisms, both the intraparticle diffusion model and the Elovich model, can be applied. The intraparticle diffusion model originating from Fick's second law was used [28–30]:

$$q_t = k_i t^{1/2} \quad (3)$$

The rate constant of intraparticle diffusion k_i [$\text{mg}/(\text{g h}^{1/2})$] is determined from the linear plot of q_t versus $t^{1/2}$ shown in Fig. 9. The constants k_i are listed in Table 2.

In reactions involving chemisorption of gases over solid surface without desorption of the products, the rate decreases with time due to increased surface coverage. One of the most useful

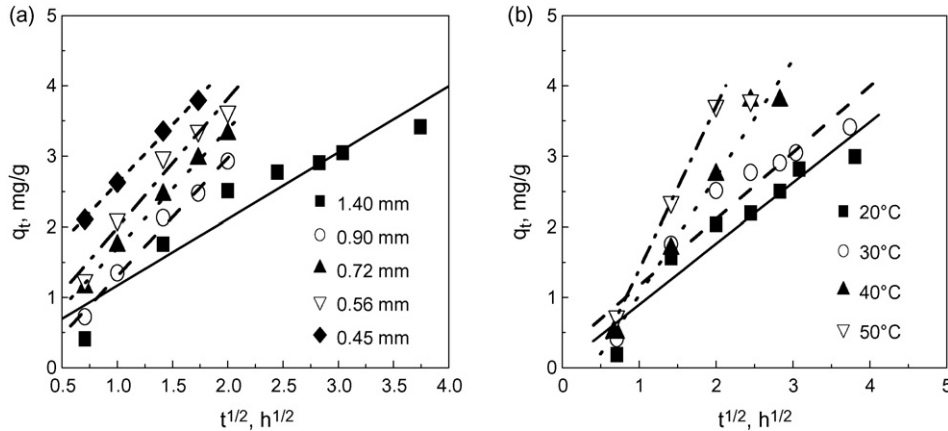


Fig. 9. Plots conforming to intraparticle diffusion model corresponds to: (a) experiments in Fig. 3 and (b) experiments in Fig. 6.

Table 2
Kinetic parameters and the standard deviations for adsorption of surfactin onto activated carbon

Particle-size (mm)	Temperature ($^{\circ}\text{C}$)	Intraparticle		Elovich		
		k_i ($\text{mg}/(\text{g h}^{1/2})$)	σ (%)	α ($\text{mg}/(\text{g h})$)	β (g/mg)	σ (%)
1.40	30	0.94	23.3	3.08	1.12	5.4
0.90	30	1.67	5.0	3.99	0.96	3.3
0.72	30	1.68	2.7	5.84	0.95	3.0
0.56	30	1.83	7.2	7.02	0.86	1.7
0.45	30	1.66	1.0	16.50	1.05	1.8
1.40	20	0.83	42.1	2.28	1.21	8.6
1.40	30	0.94	23.3	3.08	1.12	5.4
1.40	40	1.66	5.8	3.21	0.79	15
1.40	50	1.86	12.5	4.46	0.76	5.9

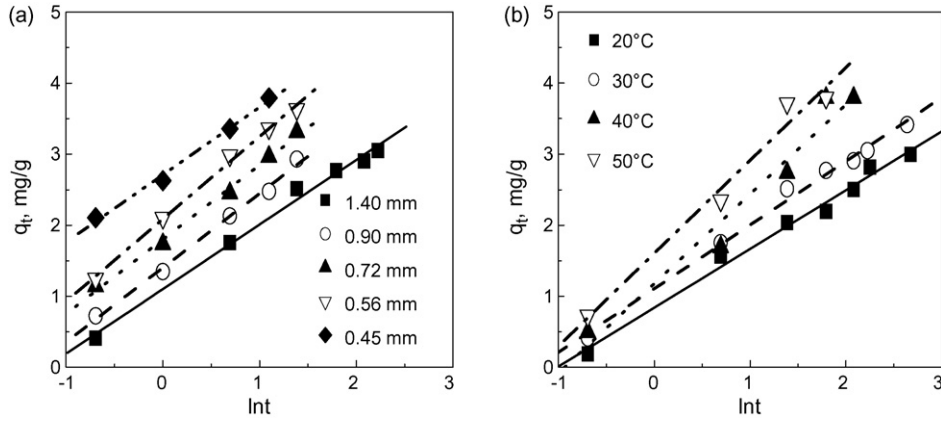


Fig. 10. Plots conforming to Elovich model corresponds to: (a) experiments in Fig. 3 and (b) experiments in Fig. 6.

models for describing such cases is Elovich one [30]:

$$\frac{dq_t}{dt} = \alpha \exp(-\beta q_t) \quad (4)$$

In this equation α is the initial adsorption rate [mg/(g h)] and β is related to the extent of surface coverage and activation energy for chemisorption (g/mg). Integration of Eq. (4) at boundary conditions similar to the pseudo-first-order equation yields

$$q_t = \left(\frac{1}{\beta}\right) \ln(t + t_0) - \left(\frac{1}{\beta}\right) \ln t_0 \quad (5)$$

where $t_0 = 1/\alpha\beta$. If $t \gg t_0$, Eq. (5) is simplified to

$$q_t = \left(\frac{1}{\beta}\right) \ln(\alpha\beta) + \left(\frac{1}{\beta}\right) \ln t \quad (6)$$

Data processing relevant to Elovich equation has been carried out by plotting q_t versus $\ln t$, as shown in Fig. 10. Parameter t_0 was determined by trial and error procedure in a way as to ensure that q_t versus $\ln(t + t_0)$ follows a straight line. Parameter β was obtained from the slope of the line, and the initial rate α was then calculated substituting t_0 and β values [20]. These data is also listed in Table 2. It should be noted that under the studied conditions the values obtained for $t_0 (=1/\alpha\beta)$ are in the range 0.05–0.4 h. Hence, the assumption $t \gg t_0$ for Eq. (6) was reasonably valid. The standard deviation σ between the experimental and the calculated results is defined as:

$$\sigma (\%) = \frac{1}{N} \sum_{i=1}^N \left| \frac{q_{t,\text{exp}} - q_{t,\text{cal}}}{q_{t,\text{exp}}} \right| \times 100 \quad (7)$$

Since using mechanistic analysis both models represent adequately the experimental data (see Figs. 9 and 10 and Table 2), the adsorption mechanisms cannot be identified clearly. It is interesting to find that Elovich equation fits the experimental data better than the intraparticle diffusion model does. This testing suggests that the chemisorption (chemical reaction) mechanism is likely to be rate controlling in the present process. Since physical adsorption and, also in more cases, chemisorption, is an exothermic process, it could be expected that an increase in temperature of the adsorbate–adsorbent system would result in decreased sorption capacity. It is shown in this work that with

temperature rise, the adsorption capacity of the activated carbon (AC) decreases, however, the adsorption rate becomes faster (Figs. 5 and 6). The adsorption rate rise indicates that, first, the diffusion process (intraparticle transport-pore diffusion), being an endothermic process, may be rate-controlling. However, if the chemisorption step is endothermic, the rate-controlling step may be attributed to the chemisorption. Additional data, from thermodynamical and chemical analysis are needed in order to be able to identify clearly the adsorption mechanism.

4. Conclusions

Adsorption from aqueous solutions of surfactin by using activated carbon has been studied. The following has been inferred:

1. The activated carbon (AC) Merck (Ref. 1.02514.1000) performs as an effective adsorbent for surfactin recovery from the model medium. The adsorption is tested by using AC of different particle-size, e.g. 1.40, 0.90, 0.72, 0.56 and 0.45 mm. The smaller the activated particles used, the faster the adsorption rate was.
2. Referring to the range of agitation rates between 80 and 180 rpm, the data obtained indicate that the external transport is too fast to represent the rate-limiting step of the overall adsorption.
3. A pH range of 6.5–8.5 and a temperature of 30 °C are found optimal for the adsorption. The adsorption was effective even in a wide pH range of 6.5–8.5, which implies that the culture medium proposed can be used directly for surfactin recovery.
4. The equilibrium between surfactin in solution and on the adsorbent surface and the adsorption rates depend strongly on temperature.

References

- [1] K. Arima, A. Kakinuma, G. Tamura, Surfactin, a crystalline peptidolipid surfactant produced by *Bacillus subtilis*: isolation, characterization and its inhibition of fibrin clot formation, *Biochem. Biophys. Res. Commun.* 31 (1968) 488–494.
- [2] M. Osman, Y. Ishigami, K. Ishikawa, Y. Ishizuka, H. Holmsen, Dynamic transition of α -helix to β -sheet structure in linear surfactin correlating to critical micelle concentration, *Biotechnol. Lett.* 16 (1994) 913–918.

- [3] F. Peypoux, J.M. Bonmatin, J. Wallach, Recent trends in the biochemistry of surfactin, *Appl. Microbiol. Biotechnol.* 51 (1999) 553–563.
- [4] C.N. Mulligan, Environmental applications for biosurfactants, *Env. Pollut.* 133 (2005) 183–198.
- [5] J.D. Desai, I.M. Banat, Microbial production of surfactants and their commercial potential, *Microbiol. Mol. Biol. Rev.* 61 (1997) 47–64.
- [6] I.M. Banat, Biosurfactants production and possible uses in microbial enhanced oil recovery and oil pollution remediation: a review, *Bioresour. Technol.* 51 (1995) 1–12.
- [7] C.N. Mulligan, R.N. Yong, B.F. Gibbs, Surfactant-enhanced remediation of contaminated soil: a review, *Eng. Geol.* 60 (2001) 371–380.
- [8] S.C. Lin, Biosurfactants: recent advances, *J. Chem. Technol. Biotechnol.* 66 (1996) 109–120.
- [9] K.D. Schaller, S.L. Fox, D.F. Bruhn, K.S. Noah, G.A. Bala, Characterization of surfactin from *Bacillus subtilis* for application as an agent for enhanced oil recovery, *Appl. Biochem. Biotechnol. Part A: Enzyme Eng. Biotechnol.* 115 (2004) 827–836.
- [10] D.A. Davis, H.C. Lynch, J. Varley, The production of surfactin in batch culture by *Bacillus subtilis* ATCC 21332 is strongly influenced by the conditions of nitrogen metabolism, *Enzyme Microb. Technol.* 25 (1999) 322–329.
- [11] M.S. Yeh, Y.H. Wei, J.Sh. Chang, Enhanced production of surfactin from *Bacillus subtilis* by addition of solid carriers, *Biotechnol. Prog.* 21 (2005) 1329–1334.
- [12] Y.H. Wei, I.M. Chu, Mn^{2+} improves surfactin production by *Bacillus subtilis*, *Biotechnol. Lett.* 24 (2002) 479–482.
- [13] K. Arima, A. Kakinuma, A. Tamura, Surfactin, a crystalline peptidelipid surfactant produced by *Bacillus subtilis*: isolation, characterization and its inhibition of fibrin clot formation, *Biochem. Biophys. Res. Commun.* 31 (1968) 488–494.
- [14] D.A. Davis, H.C. Lynch, J. Varley, The application of foaming for the recovery of surfactin from *B. subtilis* ATCC 21332 cultures, *Enzyme Microb. Technol.* 28 (2001) 346–354.
- [15] S.Ch. Lin, H.J. Jiang, Recovery and purification of the lipopeptide biosurfactant of *Bacillus subtilis* by ultrafiltration, *Biotechnol. Tech.* 11 (1997) 413–416.
- [16] R. Sen, T. Swaminathan, Characterization of concentration and purification parameters and operating conditions for the small-scale recovery of surfactin, *Process Biochem.* 40 (2005) 2953–2958.
- [17] K. Schügerl, J. Hubbuch, Integrated bioprocesses, *Curr. Opin. Microbiol.* 8 (2005) 294–300.
- [18] P.D. Purakayastha, A. Pal, M. Bandyopadhyay, Sorption kinetics of anionic surfactant on to waste tire rubber granules, *Sep. Purif. Technol.* 46 (2005) 129–135.
- [19] J.S. Zogorski, S.D. Faust, J.H. Hass Jr., The kinetics of adsorption of phenols by granular activated carbon, *J. Colloid Interface Sci.* 55 (1976) 329–341.
- [20] W.J. Weber Jr., F.L. Slejko (Eds.), *Adsorption Theory, Concepts and Models*, Marcel Dekker, NY, 1985.
- [21] L.D. Benefield, J.F. Judkins, B.L. Eeand, *Process Chemistry for Water and Wasterwater Treatment*, Prentice-Hall Inc., NJ, 1982.
- [22] D.G. Cooper, C.R. MacDonald, S.J.B. Duff, N. Kosaric, Enhanced production of surfactin by continuous product removal and metal cation additions, *Appl. Env. Microbiol.* 42 (1981) 408–412.
- [23] E. Akpa, P. Jacques, B. Wathelet, M. Paquot, R. Fuchs, H. Budzikiewicz, P. Thonart, Influence of culture conditions on lipopeptide production by *Bacillus subtilis*, *Appl. Biochem. Biotechnol. Part A: Enzyme Eng. Biotechnol.* 91 (2001) 551–561.
- [24] H. Razafindralambo, M. Paquot, C. Hbid, P. Jacques, J. Destain, P. Thonart, Purification of antifungal lipopeptides by reversed phase high-performance liquid chromatography, *J. Chromatogr.* 639 (1993) 81–85.
- [25] K. Oka, T. Hirano, M. Homma, H. Ishii, K. Murakami, S. Mogami, A. Motizuki, H. Morita, K. Takeya, H. Itokawa, Satisfactory separation and MS–MS spectrometry of six surfactin isolated from *Bacillus subtilis* natto, *Chem. Pharm. Bull.* 41 (1993) 1000–1002.
- [26] I. Nikov, M. Martinov, F. Gancel, Ph. Jacques, S.D. Vlaev, Influence de la surfactine sur le transfert d’oxygène et la formation de mousse en bioréacteur, SFGP, in press.
- [27] K.D. Danov, P.M. Vlahovska, T. Horozov, C.D. Dushkin, P.A. Kralchevsky, A. Mehreteab, G. Broze, Adsorption from micellar surfactant solutions: nonlinear theory and experiment, *J. Colloid Interface Sci.* 183 (1996) 223–235.
- [28] R.S. Juang, F.C. Wu, R.L. Tseng, Mechanism of adsorption of dyes and phenols from water using activated carbons prepared from plum kernels, *J. Colloid Interface Sci.* 227 (2000) 437–444.
- [29] Y.S. Ho, G. McKay, Comparative sorption kinetic studies of dye and aromatic compounds onto fly ash, *J. Env. Sci. Health A* 34 (1999) 1179–1204.
- [30] M.Y. Chang, R.S. Juang, Equilibrium and kinetics studies on the adsorption of surfactant, organic acids and dyes from water onto natural biopolymers, *Colloid Surf. A: Physicochem. Eng. Aspects* 269 (2005) 35–46.